Journal of ELECTRONIC MATERIALS, Vol. 47, No. 8, 2018
https://doi.org/10.1007/s11664-018-6312-8

TOPICAL COLLECTION: ELECTRONIC MATERIALS FOR RENEWABLE ENERGY APPLICATIONS

The Type-2 Fuzzy Logic Controller-Based Maximum Power Point Tracking Algorithm and the Quadratic Boost Converter for Pv System

NECMI ALTIN [1,2]

1.—Department of Electrical-Electronics Engineering, Faculty of Technology, Gazi University, Teknikokullar, 06500 Ankara, Turkey. 2.—e-mail: naltin@gazi.edu.tr

An interval type-2 fuzzy logic controller-based maximum power point tracking algorithm and direct current–direct current (DC–DC) converter topology are proposed for photovoltaic (PV) systems. The proposed maximum power point tracking algorithm is designed based on an interval type-2 fuzzy logic controller that has an ability to handle uncertainties. The change in PV power and the change in PV voltage are determined as inputs of the proposed controller, while the change in duty cycle is determined as the output of the controller. Seven interval type-2 fuzzy sets are determined and used as membership functions for input and output variables. The quadratic boost converter provides high voltage step-up ability without any reduction in performance and stability of the system. The performance of the proposed system is validated through MATLAB/Simulink simulations. It is seen that the proposed system provides high maximum power point tracking speed and accuracy even for fast changing atmospheric conditions and high voltage step-up requirements.

Key words: Quadratic boost converter, interval type-2 fuzzy logic controller, MPPT, PV system

INTRODUCTION

With growing world energy demand, increasing awareness of environmental issues, energy security and reliability, research on renewable energy sources has been increasing. As a result of these studies, solar energy and wind energy seem more attractive than others. Photovoltaic (PV) systems which convert photo-energy into electrical energy directly by using PV cells and modules have received great attention. PV systems are modular in nature and generate direct current (DC) electrical energy without any fuel cost. In addition, since they do not have any dynamic parts, their maintenance cost is very low and they have la ong life. Therefore, PV systems have widespread use in different applications and at different power levels, such as large-scale power plants, home applications, water pumping, street lightning, telecommunication transmitters, vehicle applications, space applications, etc.[1,2] A PV module cannot be modeled as a constant DC current source because its output changes with parameters such as load current, temperature, irradiation level, etc. It has a current–voltage (I–V) characteristic under constant and uniform solar irradiance and temperature. The PV module generates maximum power and operates with maximum energy conversion efficiency at a unique point on this I–V curve for constant temperature and solar irradiation level. This point is called the maximum power point (MPP), and continuously tracking this MPP of a PV array is required to obtain maximum efficiency.[1]

Many maximum power point tracking (MPPT) algorithms have been proposed for PV systems. These algorithms can be grouped into two categories, as direct and indirect methods. Indirect

(Received November 27, 2017; accepted April 18, 2018; published online May 3, 2018)

methods use some offline measurements, predefined equations and models to determine the MPP, and are therefore also called offline methods. Constant voltage, constant current, and pilot cell are common indirect methods. Some issues such as aging and the dirtiness of the module surface affect the performance of the system. Although these methods have fast responses, they are not guaranteed to track the real MPP. Therefore, direct methods have been proposed. These methods use online measurements to track the MPP of a PV system. Perturb and observe (P&O) is a well-known and simple MPPT algorithm. It is also combined with soft switching applications to achieve higher efficiency values.[3] This algorithm generates a perturbation and then monitors the PV power. According to the variation of the PV power, the next control signal is determined. This method is simple; but there is a natural oscillation around the MPP. In addition, its response is related to the perturbation step size. While the small values of the perturbation step size worsen the response time and decrease the oscillation around the MPP, larger values improve the response time but cause large oscillations around the MPP.[4–6] The increment conductance (IC) algorithm is another common direct MPPT method. This method monitors the slope of the PV power versus PV voltage (P–V) curve. The slope of this curve is zero at the MPP, and has positive and negative values at the right and left sides of the MPP, respectively. The oscillations around the MPP are reduced in this method but tracking speed is still related to the step size. Therefore, some modifications have been proposed for both the P&O and the IC algorithms to provide a variable step size.[6,7] Artificial neural networks (ANN) are also used as MPPT algorithms. ANNs have a unique advantage in that they can be educated with real values. However, these can also be considered for MPPT applications, which make algorithms effective for only certain module types used in education. In addition, aging and other parameter decays in time reduce the performance of the algorithm.[7,8] Although monitoring cells can be used to modify ANN-based MPPT algorithms and to remove these effects, this increases the cost and reduces the total system efficiency.[9]

The fuzzy logic controller (FLC), which does not require an exact model of the system and has a robust performance, is also used as a MPPT algorithm. Different input and output variables, different membership functions and different inference methods have been used for FLC-based MPPT algorithms. These algorithms provide considerably higher performance and tracking speed. However, the performance of the algorithm is greatly affected by the experience and knowledge of the designer. If the designer determines the optimum membership functions and rules, the FLC-based MPPT algorithm has a very good performance, otherwise its performance may be moderate. Designers usually determine these parameters bywith trial and error, using their experience. This defines some uncertainties in the rules and membership functions of the FLC, which may deteriorate the performance.[7]

Conventional FLC and fuzzy sets, now called type-1 fuzzy sets (T-1FSs), have been extended by Zadeh, and new concept called type-2 fuzzy sets (T-2FSs) have been introduced.[10] In these new sets, a third dimension is added to handle the aforementioned uncertainties. Therefore, many research studies have been proposed based on T-2FSs, such as control of power electronics converters, motor drives, robotic systems, motion control systems, etc.[11–16] Since the T2-FSs are useful for handling uncertainties such as noisy data and changing environmental conditions, they have also been applied to PV systems,[17,18] and type-2 fuzzy logic-based MPPT algorithms have been proposed, but these applications are mainly based on conventional buck or boost converters.[19]

The DC voltage generated by the PV module varies with environmental conditions and load. This varying voltage should be regulated to supply loads. In addition, load power should be regulated to track the MPP from PV module. Therefore, DC–DC converters such as buck, boost and buck–boost converters according to input–output voltage relationships can be used in PV systems. Since the voltage levels of the PV modules are low, boost converters are commonly used to step up the PV voltage. Although the voltage gain of the boost converter increases with duty cycle, higher duty cycle values decrease the stability and increase the control difficulty. Therefore, the practical voltage gain of the boost converter is limited and recommended to be selected as a maximum of four.[20,21] A number of PV modules should be connected in series to fulfill the voltage requirement, whereas the number of series-connected PV modules must in practice be within certain limits due to limitations on PV voltage isolation, efficiency, shadowing effect, etc. Consequently, some new DC–DC converter topologies have been proposed to provide higher voltage conversion gains. Although the isolated DC–DC converter topologies remove this limitation, they cause some problems, such as cost, complexity, etc.[22]

Different converter topologies have been proposed to obtain high voltage conversion gain with high efficiency. Initial studies have been based on extensions of the conventional boost converter to increase its voltage conversion gain. The conventional boost converter combined with a switched capacitor has been proposed. Here, voltage conversion gain is related to the number of capacitors used in the circuit. Since the voltage regulation action significantly decreases the efficiency of the converter, an additional converter is required to combine the high voltage conversion gain and voltage regulation features with high efficiency.[23] In addition, the power switches suffer from high charge currents.

DC–DC multilevel boost converter topology is proposed to remove this additional converter requirement. This topology also combines the boost converter and the switched capacitor. Several capacitors are charged with the same voltage through the conventional boost converter.[24] This removes the voltage regulation problem. However, the total load current flows through the output capacitors and this limits the usage of this topology.[20]

Using coupled inductors with conventional boost converters is another technique used to achieve high voltage conversion gain.[25] However, the leakage inductor energy of the coupled inductors causes voltage spikes which increase switching losses and decreases the efficiency.[26] Although active and passive clamp circuits are designed to recycle the leakage inductor energy, these additional clamp circuits increase the cost and complexity of the system.[20] High voltage conversion gain can be obtained by cascaded connection of two boost converters. However, this topology doubles the numbers of required components and controllers. The quadratic boost converter (QBC) shown in Fig. 1 is similar to two cascaded boost converters and provides the same voltage conversion ratio with only one active switch and one controller. The output voltage is given as a quadratic function of the duty cycle of the switching signal.[27] Since the QBC has only one active switch, additional active switch and driver circuit requirements are removed and a more reliable and efficient converter is obtained. Therefore, the QBC has become popular and is used in different DC–DC converter applications such as power factor correction applications and PV applications.[28–30] The output voltage of the fuel cell or PV module is usually low, and this low voltage should be increased to supply conventional AC loads or to export generated energy to the grid. Therefore, a compact, robust, reliable and high-efficiency converter design with a high voltage conversion ratio is an important requirement for PV- and fuel cell-supplied systems. Although some studies have been presented on the control of the QBC, the number of studies on MPPT quadratic boost converters is limited.[28,31,32]

In this study, a QBC with MPPT capability is proposed for PV systems. An interval type-2 fuzzy logic controller (IT-2FLC) is used as the MPPT algorithm. Thus, the high voltage step-up functions of the QBC and the high tracking speed and MPPT accuracy properties of the IT-2FLC are combined. The performance of the proposed system has been verified by MATLAB/Simulink simulations. The proposed IT-2FLC-based MPPT algorithm determines the system operation point, which varies with load, solar irradiation and temperature variations, and tracks the MPP of the PV system with high speed and accuracy. The simulation results show that the proposed IT-2FLC based MPPT method exactly tracks the MPP of the PV system and has a fast transient response. It is seen that the proposed MPPT method is especially suitable for rapidly changing atmospheric conditions.

PV EQUIVALENT CIRCUIT

The PV cell is the main part of the PV system. PV modules are generated by parallel or/and serial connections of PV cells. PV cells consist of a semiconductor material which is formed in a p–n junction similar to a diode. The equivalent circuit of the ideal PV cell is given in Fig. 2.[33] The solar light load excites the free electrons when it contacts the cell surface. If the output of the PV cell is loaded or short-circuited, a photo-current is generated by these free electrons. PV cell manufacturers determine certain parameters and nonlinear I–V characteristics as a result of test reports. The mathematical model of a PV cell can be derived by using these parameters. The PV cell output current can be written as:

$$I = I_{\text{pv\_cell}} - I_{0\_\text{cell}}\left[\exp\left(\frac{q.V}{a.k.T}\right) - 1\right], \tag{1}$$

$$I = I_{\text{pv\_cell}} - I_{\text{d}}, \tag{2}$$

where $I_{\text{pv\_cell}}$ is the generated photocurrent, I_{d} the diode current, I_{0_cell} the diode reverse saturation current (A), q the electron charge, k the Boltzman's constant, T is the cell (p–n junction) temperature

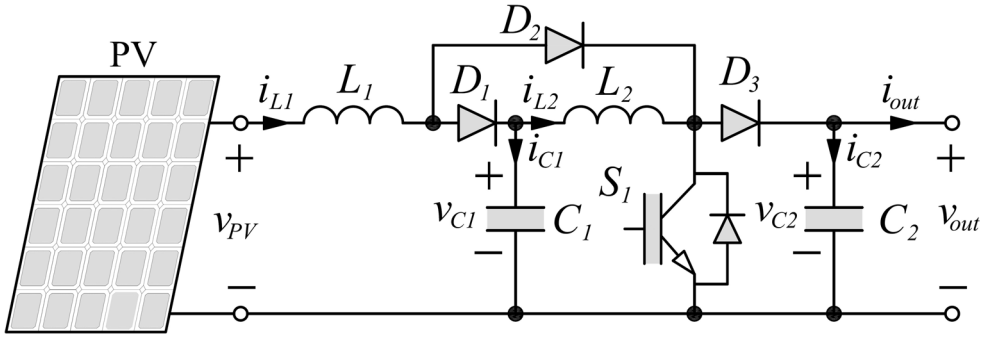

Fig. 1. The PV-supplied quadratic boost converter.

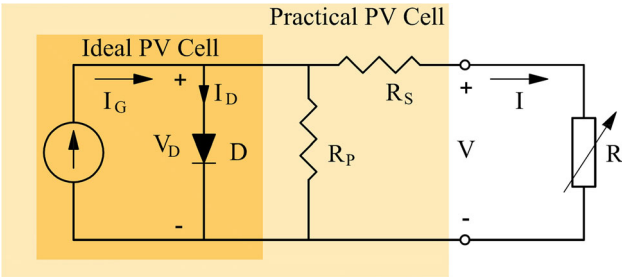

Fig. 2. Equivalent model of a PV cell.

(K), and a an ideal p–n junction characteristics factor.[34]

Equation 1 is valid for an ideal PV cell, but it may cause errors for real applications. All time variant parameters of a PV system should be added to the model to prevent wrong calculations. Also, a number of PV cells are connected in series or parallel to increase the output voltage, current and power level, and thus the PV module is obtained. So, the output current of a PV module can be written as[35]:

$$I = I_{\mathrm{pv}} - I_0\left[\exp\left(\frac{V + IR_{\mathrm{s}}}{aV_{\mathrm{t}}}\right) - 1\right] - \left(\frac{V + IR_{\mathrm{s}}}{R_{\mathrm{p}}}\right), \quad (3)$$

$$V_{\mathrm{t}} = \frac{kN_{\mathrm{S}}T}{q} \quad (4)$$

$$I_{\mathrm{pv}} = I_{\mathrm{pv\_cell}} \cdot N_{\mathrm{p}} \quad (5)$$

$$I_0 = I_{0\_\mathrm{cell}} \cdot N_{\mathrm{p}} \quad (6)$$

where I and V are the PV module output current and voltage, respectively, I_{pv} is the generated photocurrent (A), I_0 the diode reverse saturation current (A), V_{t} the cell thermal voltage (V), R_{s} the serial resistance value of the PV cel, R_{p} the parallel resistance value of the PV cell, and N_{p} and N_{s} are the number of parallel-connected and serial-connected PV cells, respectively. I_{pv} and I_0 can be calculated with parameters given in the manufacturer's datasheet for standard test conditions (25°C temperature and 1000 W/m2 solar irradiation level). The PV module current for real-time operation conditions can be found with[34]:

$$I = \left(I_{\mathrm{pv\_n}} + K_{\mathrm{I}}.\Delta T\right)\frac{G}{G_{\mathrm{n}}}, \quad (7)$$

where ΔT is the temperature difference between the test condition and the operation condition ($\Delta T = T - T_{\mathrm{n}}$), K_{I} the short circuit current/temperature coefficient, G the irradiation level for operation condition, and G_{n} the irradiation level for the standard test condition. The diode saturation current value for real-time operation condition can be calculated with:

$$I_0 = I_{0,\mathrm{n}}\left(\frac{T_{\mathrm{n}}}{T}\right)^2 \exp\left[\frac{q \cdot E_{\mathrm{g}}}{a \cdot k} \cdot \left(\frac{1}{T_{\mathrm{n}}} - \frac{1}{T}\right)\right] \quad (8)$$

$$I_{0\_\mathrm{n}} = \frac{I_{\mathrm{sc\_n}}}{\exp\left(\frac{V_{\mathrm{oc\_n}}}{a \cdot V_{\mathrm{t\_n}}}\right) - 1}, \quad (9)$$

where $I_{\mathrm{sc\_n}}$ is short circuit current; $V_{\mathrm{oc\_n}}$ is open circuit voltage and $V_{\mathrm{t\_n}}$ is thermal voltage of N_{s} series connected PV cells at nominal test temperature.

THE QUADRATIC BOOST CONVERTER

In the literature, different quadratic converter topologies, which can be designed as buck converters or boost converters, have been proposed.[21,22,36] The efficiency of the QBC is still lower than the conventional boost converter.[36] Nevertheless, it is well known that higher duty ratios which are required to obtain higher voltage gains dramatically decrease the conventional converter efficiency and increase electromagnetic interference and the voltage stress on the switches.[26–28] Therefore, the QBC has a better performance for high-voltage step-up applications such as PV and fuel cell applications.

Analysis of the QBC shown in Fig. 1 can be easily performed. If the controlled switch S_1 is turned on (ON state), then the D_1 and D_3 diodes pass to the OFF state, and the supply current flows through L_1 and D_2. In this condition, the inductor, L_1, stores energy from the supply and the inductor, L_2, stores energy from the capacitor, C_1. Simultaneously, load is supplied by the output capacitor, C_2. Then, the switch, S_1, turns off (OFF state). In this condition, the diode states are completely contrary: D_1 and D_3 are in the ON state, and D_2 is in the OFF state. At the same time, the C_1 and C_2 capacitors are charged by the L_1 and L_2 inductors. In addition, the inductors supply the load energy demand. The equation of the converter voltage conversion ratio can be obtained from differential equations according to the control signal (u).[29] Equations 10–13 can be written for capacitor voltages and inductor currents:

$$\frac{\mathrm{d}i_{L_1}}{\mathrm{d}t} = \frac{v_{\mathrm{pv}}}{L_1} - \frac{v_{C_1}}{L_1}(1-u) \quad (10)$$

$$\frac{\mathrm{d}i_{L_2}}{\mathrm{d}t} = \frac{v_{C_1}}{L_2} - \frac{v_{C_2}}{L_2}(1-u) \quad (11)$$

$$\frac{\mathrm{d}v_{C_1}}{\mathrm{d}t} = -\frac{i_{L_2}}{C_1} + \frac{i_{L_1}}{C_1}(1-u) \quad (12)$$

$$\frac{\mathrm{d}v_{C_2}}{\mathrm{d}t} = -\frac{v_{C_2}}{RC_2} + \frac{i_{L_2}}{C_2}(1-u) \quad (13)$$

where u is the control signal, which is 1, when S_1 is turned on (ON state), and 0 when S_1 is turned off (OFF state). Here, R is the load resistance. State equations of the QBC for $X_1 = i_{L_1}, X_2 = i_{L_2}, X_3 = v_{C_1}$ and $X_4 = v_{C_2}$ can be written in state-space form as follows:

$$\begin{aligned} \dot{x} &= Ax + Bu \\ y &= Cx \end{aligned} \tag{14}$$

$$\begin{bmatrix} \dot{X}_1 \\ \dot{X}_2 \\ \dot{X}_3 \\ \dot{X}_4 \end{bmatrix} = \begin{bmatrix} 0 & 0 & -\frac{(1-u)}{L_1} & 0 \\ 0 & 0 & \frac{1}{L_2} & -\frac{(1-u)}{L_2} \\ \frac{(1-u)}{C_1} & -\frac{1}{C_1} & 0 & 0 \\ 0 & \frac{(1-u)}{C_2} & 0 & -\frac{1}{RC_2} \end{bmatrix} \begin{bmatrix} X_1 \\ X_2 \\ X_3 \\ X_4 \end{bmatrix} + \begin{bmatrix} \frac{1}{L} \\ 0 \\ 0 \\ 0 \end{bmatrix} V_{pv} \tag{15}$$

$$y = \begin{bmatrix} 0 & 0 & 0 & 1 \end{bmatrix} \begin{bmatrix} X_1 \\ X_2 \\ X_3 \\ X_4 \end{bmatrix} \tag{16}$$

In steady state conditions, all the derivative terms are equal to zero. Equation 17 is obtained by substituting the control signal D instead of u in Eqs. 10–13:

$$\frac{v_{C_1}}{v_{\text{pv}}} = \frac{v_{C_2}}{v_{C_1}} = \frac{1}{1-D} \tag{17}$$

Finally, the conversion ratio of the converter ($M(D)$) can be obtained from:

$$M(D) = \left(\frac{v_{C_1}}{v_{\text{pv}}}\right)\left(\frac{v_{C_2}}{v_{C_1}}\right) = \frac{1}{(1-D)^2} \tag{18}$$

It can be seen from Eq. 18 that the conversion ratio of the QBC is an exponential expression which provides a high conversation ratio even with a lower duty cycle.

TYPE-2 FUZZY LOGIC CONTROLLERS

The FLC, which is one of the most common applications of fuzzy sets and systems, has some advantages such as being nonlinear and adaptive in nature, combining information of experts with measurements and system models, providing robust performance under parameter variation and load disturbances, removing the requirement of accurate mathematical models of the plant. etc. Latest improvements in microprocessors and field-programmable gate arrays make them more popular.[37] However, the FLC must overcome uncertainties because of the many different sources: noisy sensor measurements, variation of sensor measurements with environmental conditions such as temperature, humidity, etc., and different opinions of experts on the same topic, while variable meanings of words used by different people are the most common uncertainties. Also, aging of the PV modules may be a reason of some uncertainties. Since membership functions of the T-1FSs are crisp, these uncertainties turn into uncertainties about the membership of T-1FSs.

The T-2FSs are an extension of T-1FSs. While the membership grade of T-1FSs are crisp numbers in [0,1], the T-2FSs are characterized by a fuzzy membership function and these membership functions have fuzzy grades of membership, i.e., a fuzzy set in [0,1]. The membership functions of T-2FSs are depicted in Fig. 3. In Fig. 3a and b, triangular type-2 fuzzy sets with blurring of the width and blurring of the center of triangular T-1FSs are shown, respectively. The membership function can be written as:

$$\tilde{\mu}(x) = \begin{cases} 1 - \frac{|x-c|}{d} & \text{if } c-d<x<c+d \\ 0 & \text{else} \end{cases} \tag{19}$$

where x is the input vector, and c and d are the center point and the width of the membership function, respectively.[35]

As seen from the figure, the membership functions of T-2FSs are three-dimensional, unlike T-1FSs which are characterized by two-dimensional membership functions. The footprint of uncertainty is the new third dimension of T-2FSs. This new third dimension allows directly modeling and handling of uncertainties.[11–15,33,38] In addition, using three-dimensional fuzzy sets facilitates the design process when determining the exact membership functions is difficult, and has the ability for modeling more sophisticated input–output relationships.

The type-2 FLCs have robust structures and a higher disturbance rejection capability against the external disturbances and noise. Based on Zadeh's idea, different T-2FSs have been presented. However, the T-2FSs cause a significant increase of the computational burden. As a result of research activities to reduce this computational burden,

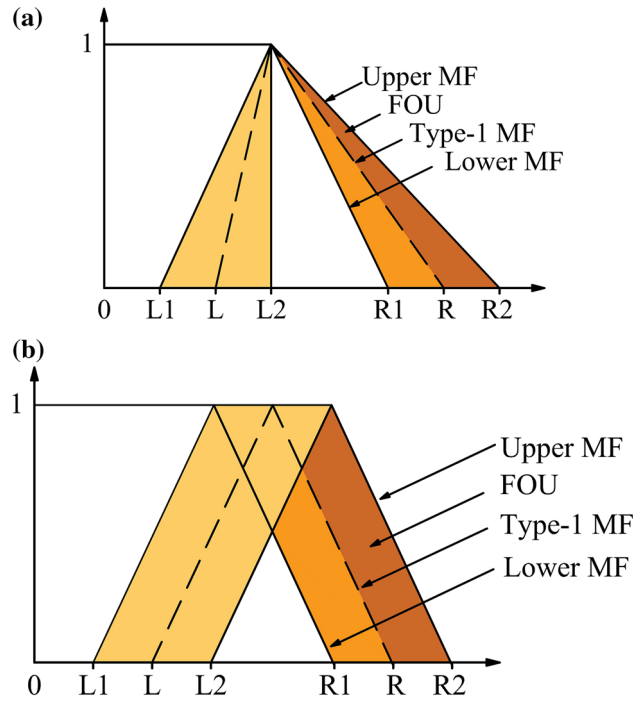

Fig. 3. Type-2 fuzzy sets (a) with blurring width of triangular type-1 fuzzy set, (b) with blurring the center of triangular type-1 fuzzy set.

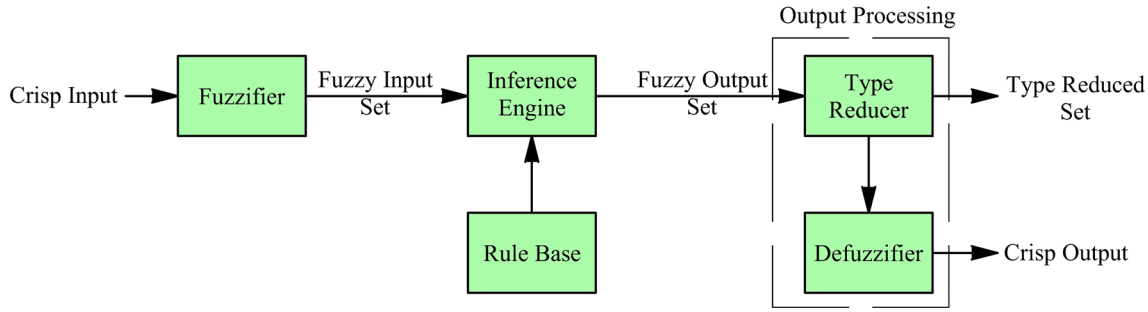

Fig. 4. General block diagram of T-2FS.

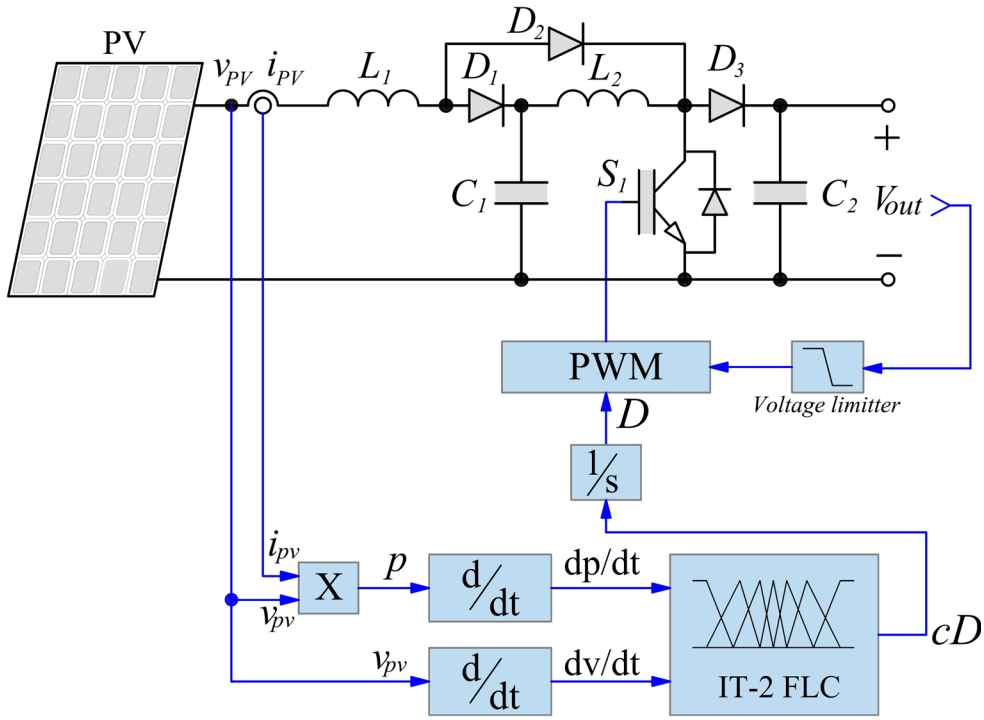

Fig. 5. Block diagram of the proposed PV system.

interval type-2 fuzzy sets, which are a simple version of type-2 fuzzy sets, are proposed. The secondary membership function of the interval type-2 fuzzy sets is not fuzzy, and therefore the execution time of these sets is shorter. The general block diagram of the interval type-2 FLC is given in Fig. 4. As it can be seen from this block diagram, an interval type-2 fuzzy system is similar to the type-1 fuzzy system except for the output-processing block, which is composed of a type reducer and a defuzzifier following it. Since membership functions are T-2FSs, the output of the inference engine is also type-2. Therefore, before the defuzzifier unit, a type reducer is used to convert output signals from T-2FSs to T-1FSs. Then, the defuzzifier converts T-1FSs to crisp output values.[11–15,33,38]

The principle of type-2 FLCs is very much like the type-1 FLCs. The fuzzifier maps crisp inputs to T-2FS. The general structure for both type-1 fuzzy logic systems and type-2 fuzzy logic systems is the same. The only difference is that the antecedents and the consequents of type-2 fuzzy logic systems are represented as T-2FSs. The inference engine combines the rules and produces output T-2FSs from input T-2FSs. The type reducer generally reduces the T-2FSs into T-1FSs which is then converted to a crisp output through the defuzzifier. Finally, a crisp output is obtained.[36]

PROPOSED IT-2FLC BASED MPPT ALGORITHM

In this study, a MPPT system including MPPT algorithm and power electronics converter has been designed. The QBC that has same voltage step-up ability with a cascaded boost converter is used as the power converter. Thus, high voltage conversion gain is obtained with only one active switch. The IT-

2FLC based MPPT algorithm is also designed to track the MPP of the PV system which is affected by operation conditions, irradiation level and temperature. The block diagram of the proposed system is depicted in Fig. 5.

The IT-2FLCs have two inputs and one output. The change in PV module power (dP/dt) and the change in PV voltage (dv_{pv}/dt) are used as input variables and the change in duty cycle (cD) is used as the output variable. Seven membership functions for both input and output variables have been designed, as shown in Fig. 6. The membership functions are labeled with linguistic variables, i.e., negative large (NL), negative medium (NM), negative small (NS), zero (Z), positive small (PS), positive medium (PM) and positive large (PL). The rules of the proposed IT-2FLC-based MPPT algorithm are

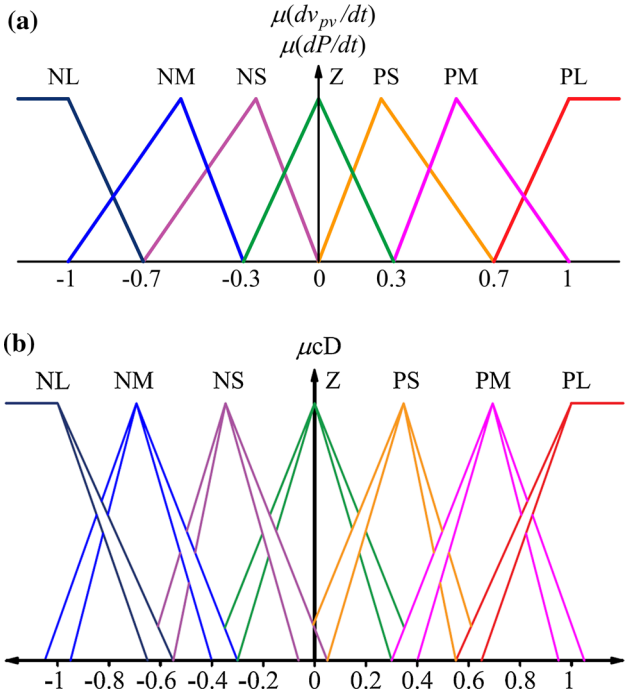

Fig. 6. (a) Membership functions for input variables dP/dt and dv_{pv}/dt. (b) Memebership functions for output variable cD.

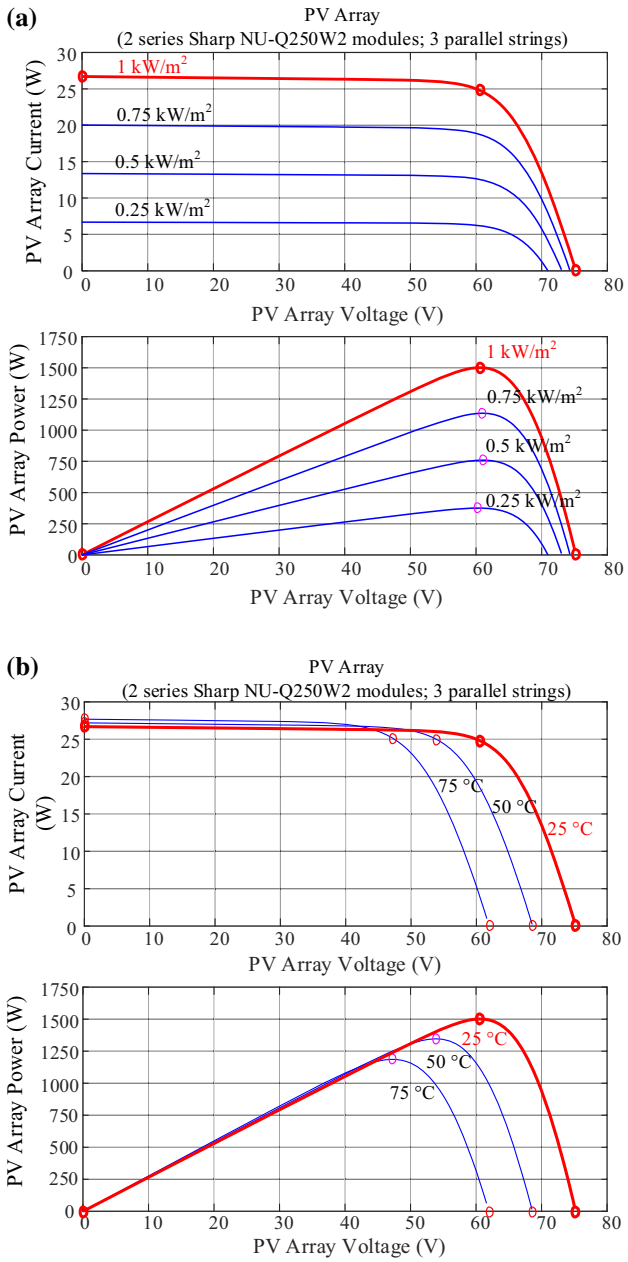

Fig. 7. Characteristics of the PV array for different (a) irradiation levels and (b) temperatures.

Table I. The rule base of the proposed IT-2FLC

dv_{pv}/dt / dP/dt	NL	NM	NS	Z	PS	PM	PL
NL	NL	NL	NM	Z	PM	PL	PL
NM	NL	NM	NM	Z	PM	PM	PL
NS	NM	NM	NS	Z	PS	PM	PM
Z	Z	Z	Z	Z	Z	Z	Z
PS	PM	PS	PS	Z	NS	NS	NM
PM	PL	PM	PM	Z	NS	NM	NL
PL	PL	PL	PM	Z	NM	NM	NL

NL negative large, *NM* negative medium, *NS* negative small, *Z* zero, *PS* positive small, *PM* positive medium, *PL* positive large.

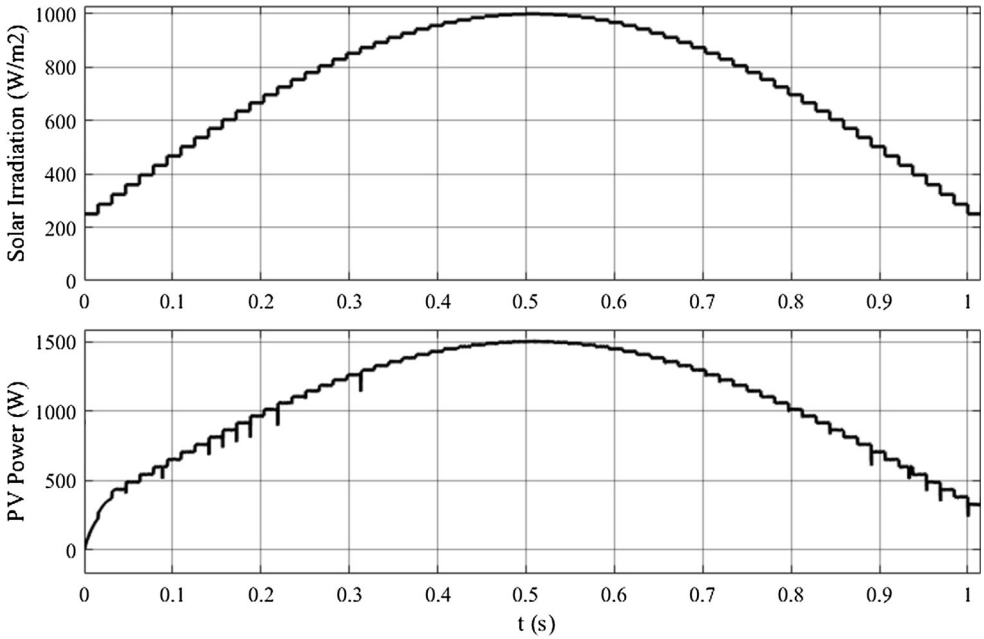

Fig. 8. Variation of output power and solar irradiation level.

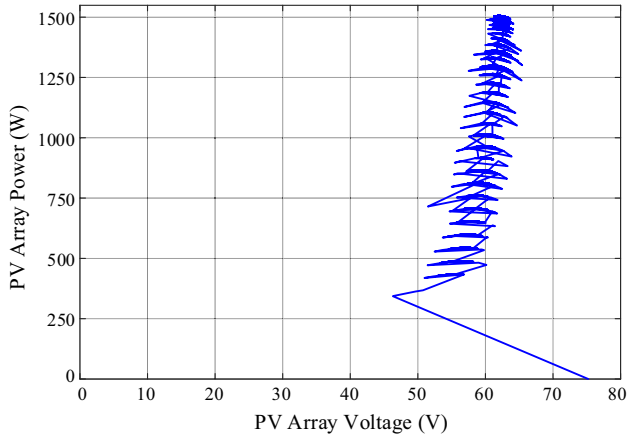

Fig. 9. *I–V* curve of the PV system while the solar irradiation level is changed from 150 W/m^2 to 1000 W/m^2.

also given in Table I. The PV array voltage and the current are measured continuously and the PV module power is calculated by using these measurements. Thus, both two inputs of the FLC are obtained. These inputs are fuzzified with input membership functions, and then the fuzzy inference engine generates the controller signal according to the input values, membership functions and rule base to track the MPP of the PV system.

After the type reducing and defuzzifying processes, crisp values of the FLC are obtained. In the literature, some methods such as centroid, center of sets, height and modified height have been proposed to use in the type reduction process.[39–41] In this study, the center of sets type-reduction method is applied. This method can be expressed as:

$$U_{\cos}(e) = [u_l, u_i] = \int_{u^1 \in [u_l^1, u_r^1]} \cdots \int_{u^M \in [u_l^M, u_r^M]} \int_{f^M \in [\underline{f}^1, \bar{f}^1]} \cdots \int_{f^M \in [\underline{f}^1, \bar{f}^1]} 1 \Big/ \frac{\sum_{i=1}^{M} f^i u^i}{\sum_{i=1}^{M} f^i} \tag{20}$$

where u_l is the left-most points, u_r the right-most points, $U_{\cos}(e)$ an interval output set determined by u_l and u_r, and i = *1*…M represents the number of rules. An iterative procedure to calculate u_l and u_r has been proposed by Karnik–Mendel.[39–41] $U_{\cos}(e)$ is generated by the type-reduction process, and the crisp output of the output variable is obtained by the averaging of u_l and u_r because these are interval variable sets[39–41]:

$$u_{\text{fuzzy}}(e) = \frac{u_l + u_r}{2} \tag{21}$$

The duty cycle value of the QBC is obtained by integrating the output of the FLC, and is used to generate PWM signals.

In this study, a proposed IT-2 FLC-based MPPT algorithm and the QBC are supplied by the PV array which are composed of three strings, and each string is obtained via series connection of two SHARP NU-Q250W2 PV modules. Some of important parameters of this PV module are given as: the module power is 250 W, the open circuit voltage of the module is 37.6 V, the short circuit current is 8.9 A, and the voltage and current values at the MPP are 30.3 V and 8.6 A, respectively. The *P–V* and *I-V* curves of the modeled PV array are given in

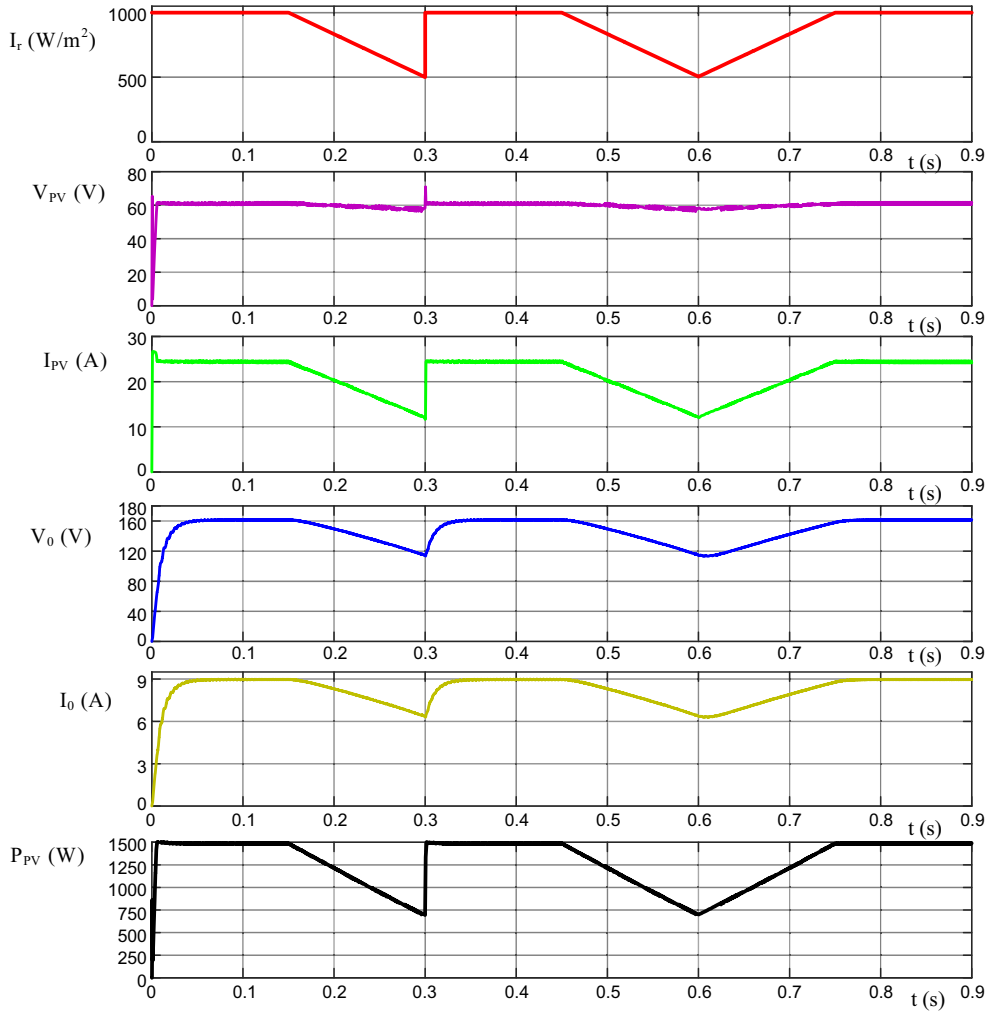

Fig. 10. The performance of the proposed MPPT algorithm and the quadratic boost converter for given MPPT patterns.

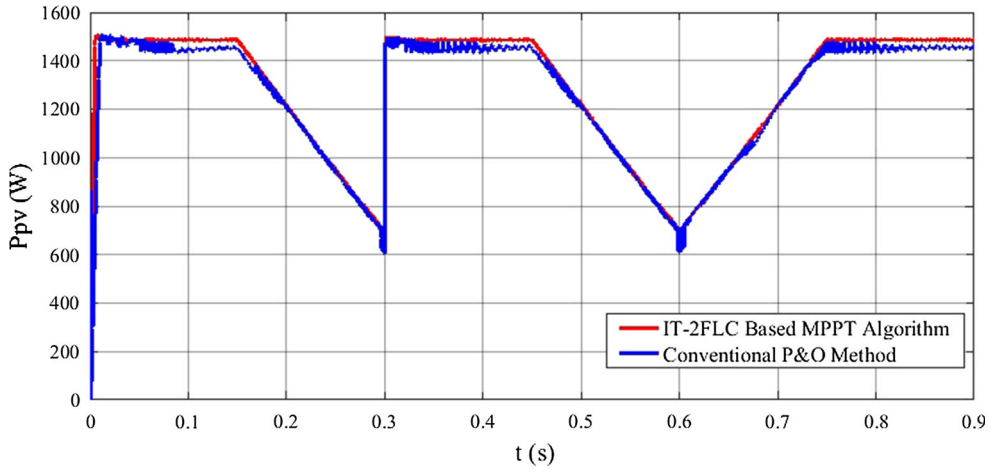

Fig. 11. Comparison of the proposed MPPT algorithm and the conventional P&O method.

Fig. 7 for different irradiation and temperature levels. The switching frequency of the converter is determined as 10 kHz.

SIMULATION RESULTS

The proposed IT-2FLC-based MPPT controller and the QBC have been modeled and then

simulated with MATLAB/Simulink. The performance of both the proposed IT-2FLC-based MPPT algorithm and the QBC have been tested with performed simulations for a 1.5-kW PV system also modeled in MATLAB/Simulink. The PV system consists of three strings composed of two serial-connected SHARP NU-Q250W2 PV modules.

The solar irradiation level is increased from 250 W/m^2 to 1000 W/m^2 step by step, and then decreased to 250 W/m^2 to test the performance of the proposed MPPT algorithm. The solar irradiation level and PV array power are depicted in Fig. 8. The proposed algorithm determines the duty cycle of the QBC according to the input variables, changes in PV array power and changes in PV voltage, and the output variable and rules of the proposed controller, and tracks the MPP of the PV system for varying solar irradiation conditions. The *P–V* graph for this operation is shown in Fig. 9. One can replace many *P–V* curves in this figure, which represents each solar irradiation level. It can be seen from these two figures that the proposed controller achieves good MPPT accuracy and tracking speed.

The variation of solar irradiation given in Fig. 8 can be referred to as a daily variation. Another solar irradiation pattern was generated to test the dynamic performance of the proposed MPPT algorithm and quadratic boost converter. This solar irradiation pattern, the PV array output voltage, the PV array current, the load voltage, the load current and the PV array power are shown in Fig. 10. As can be seen, the solar irradiation level is kept at 1000 W/m^2 until t = 0.15 s and then linearlydecreased to 500 W/m^2. At this point, a step is applied and the solar irradiation level is increased from 500 W/m^2 to 1000 W/m^2. The solar irradiation is again kept at 1000 W/m^2 until t = 0.45 s. Then, first, it is decreased to 500 W/m^2 and, second, increased to 1000 W/m^2 with the same and constant slope. It reaches 1000 W/m^2 at t = 0.75 s and tis hen kept constant. It can be easily seen that the output power of the PV array has completely the same pattern with this irradiation level. The proposed IT-2FLC-based MPPT algorithm tracks the MPP of the system even for step change conditions. It validates that the proposed algorithm has a fast transient response and high accuracy, and is suitable for rapidly changing atmospheric conditions. It is also seen from the PV system and output voltage and current waveforms that the proposed quadratic boost converter provides high voltage step-up ability without any disturbances.

The proposed MPPT algorithm is also compared with the conventional P&O method to highlight its performance. The conventional P&O method is also applied to the proposed QBC converter. Obtained results from both MPPT algorithms are depicted in Fig. 11 comparatively. It is seen that power oscillations of the P&O method are significantly removed and faster MPPT algorithm is obtained by the proposed IT-2FLC based MPPT algorithm.

CONCLUSIONS

In this study, a MPPT system for PV systems is proposed. The proposed system consists of an IT-2FLC-based MPPT algorithm and a QBC. Thus, the uncertainty-handling capability of the type-2 fuzzy systems and high voltage step-up capability of the quadratic boost converters are combined. The FLC system has two inputs, the change in PV power and the change in PV voltage, and an output variable, the change in duty cycle. The designed system is validated through MATLAB/Simulink simulations for both fast and slow irradiance variations. The results show that the proposed system has a fast response and provides high MPPT speed and accuracy even for fast irradiance changes. In addition, the proposed MPPT algorithm and the conventional P&O method are compared. It is seen that the proposed algorithm removes the oscillations significantly and provides a better dynamic response. It is also seen that the QBC, which has a quadratic output voltage equation, provides a high voltage step-up ability and removes high duty cycle requirements, and thus the robustness and stability of the system is improved. Since the proposed system requires only one active switch, a more effective and compact design is obtained.

REFERENCES

1. N. Altin and I. Sefa, *Energy Convers. Manag.* 56, 130 (2012).
2. O. Aydogmus, *Adv. Electr. Comput. En.* 12, 53 (2012).
3. S. Oncu and S. Nacar, *Int. J. Hydrogen Energy* 41, 12477 (2016).
4. I. Sefa and N. Altin, *J. Fac. Eng. Arch. Gazi Univ.* 24, 409 (2009).
5. D. Petreus, D. Moga, A. Rusu, T. Patarau, and M. Munteanu, *Adv. Electr. Comput. En.* 10, 40 (2010).
6. F. Liu, S. Duan, F. Liu, B. Liu, and Y. Kang, *IEEE Trans. Ind. Electron.* 55, 2622 (2008).
7. H. Koizumi, T. Mizuno, T. Kaito, Y. Noda, N. Goshima, M. Kawasaki, K. Nagasaka, and K. Kurokawa, *IEEE Trans. Ind. Electron.* 53, 1889 (2006).
8. Q. Mei, M. Shan, L. Liu, and J.M. Guerrero, *IEEE Trans. Ind. Electron.* 58, 2427 (2011).
9. A. Varnham, A.M. Varnham, G.S. Virk, and D. Azzi, *IEEE Trans. Energy Convers.* 22, 873 (2007).
10. J.L. Agorreta, L. Reinaldos, R. Gonzalez, M. Borrega, J. Balda, and L. Marroyo, *IEEE Trans. Ind. Electron.* 56, 4363 (2009).
11. L.A. Zadeh, *Inform. Sci.* 8, 199 (1975).
12. N.N. Karnik, J.M. Mendel, and Q. Liang, *IEEE Trans. Fuzzy Syst.* 7, 643 (1999).
13. S. Barkat, A. Tlemçani, and H. Nouri, *IEEE Trans. Fuzzy Syst.* 19, 925 (2011).
14. P.Z. Lin, C.M. Lin, C.F. Hsu, and T.T. Lee, *Proc. IEE Electr. Power Appl.* 152, 1482 (2005).
15. L. Li, W.H. Lin, and H. Liu, *Proc. Inst. Elect. Eng. Intell. Transp. Syst.* 153, 33 (2006).
16. N. Topaloglu, *Ener. Educ. Sci. Tech-A* 31, 1307 (2013).
17. A. Gheibi, S.M.A. Mohammadi, and M. Maghfoori, *Energy Procedia* 12, 538 (2011).
18. N. Altin, *Adv. Electr. Comput. En.* 13, 65 (2013).
19. I. Atacak and O.F. Bay, *J. Intel. Manuf.* 23, 1023 (2012).
20. S. Ozdemir, N. Altin, and I. Sefa, *Int. J. Hydrogen Energy* 42, 17748 (2017).
21. Y.J.A. Alcazar, D.S. Oliveira, F.L. Tofoli, and R.P. Torrico-Bascope, *IEEE Trans. Ind. Electron.* 60, 4438 (2013).

22. O. Lopez-Santos, L. Martinez-Salamero, G. Garcia, H. Valderrama-Blavi, and D. Zambrano-Prada, *IEEE Trans. Power Electron.* 32, 2253 (2017).
23. O. Abutbul, A. Gherlitz, Y. Berkovich, and A. Ioinovici, *IEEE Trans. Circuits Syst. I, Fundam. Theory Appl.* 50, 1098 (2003).
24. J.C. Rosas-Caro, J.M. Ramirez, F.Z. Peng, and A. Valderrabano, *IET Power Electron.* 3, 129 (2010).
25. B. Axelrod, Y. Berkovich, and A. Ioinovici, in *IEEE 32nd Annual Conference on Proc. Industrial Electronics, IECON*, (2006) pp. 2366–2371.
26. Y.-P. Hsieh, J.-F. Chen, T.-J. Liang, and L.-S. Yang, *IET Power Electron.* 5, 11 (2012).
27. J. Leyva-Ramos, M.G. Ortiz-Lopez, L.H. Diaz-Saldierna, and J.A. Morales-Saldana, *IET Power Electron.* 2, 605 (2009).
28. N. Altin and E. Ozturk, in *ECAI 2016—International Conference—8th Edition Electronics, Computers and Artificial Intelligence*, (2016) p. 1.
29. R. Kadri R., J.-P. Gaubert, G. Champenois, and M. Mostefaï, in *XIX International Conference on Electrical Machines (ICEM)*, (2010) pp. 1–7.
30. T. Yan., J. Xu., Z. Dong, L. Shu, and P. Yang, in *International Conference on Communications, Circuits and Systems (ICCCAS)* (2013) 2, pp. 402-406.
31. A. Ghamrawi, J.-P. Gaubert, and D. Mehdi, in *18th European Conference on Power Electronics and Applications (EPE'16 ECCE Europe)*, (2016) pp. 1–10.
32. A. Ghamrawi, J.-P. Gaubert, and D.D. Mehdi, in *IEEE International Energy Conference (ENERGYCON)*, (2016) pp. 1–6.
33. N. Altin, in *International Conference on Renewable Energy Research and Applications*, (2012) pp. 1–6.
34. M.G. Villalva, J.R. Gazoli, and E.R. Filho, *IEEE Trans. Power Electron.* 24, 1198 (2009).
35. C.A. Otieno, G.N. Nyakoe, and C.W. Wekesa, in *9th IEEE AFRICON*, (2009) pp. 1–6.
36. D.S. Wijeratne and G. Moschopoulos, *IEEE Trans. Circuits Syst. I, Reg. Papers* 59, 426 (2012).
37. S. Uzun, M.R. Canal, and N. Topaloglu, *J. Fac. Eng. Arch. Gazi Univ.* 27, 175 (2012).
38. H. Hagras, *IEEE Trans. Fuzzy Syst.* 12, 524 (2004).
39. J. Mendel, *Uncertain Rule-Based Fuzzy Logic Systems: Introduction and New directions* (Upper Saddle River: Prentice-Hall, 2001).
40. S.E. Mineiro Jr., S. Daher, F.L.M. Antunes, and C.M.T. Cruz, in *19th Annual IEEE Applied Power Electronics Conference and Exposition,* (2004) 3, pp. 1501–1506.
41. Q. Liang and J.M. Mendel, *IEEE Trans. Fuzzy Syst.* 8, 535 (2000).